The Journal of Chemical Physics

RESEARCH ARTICLE | OCTOBER 11 2023

Conditions for EPR detection of chirality-induced spin selectivity in spin-polarized radical pairs in isotropic solution

Yi Ren ; P. J. Hore

J. Chem. Phys. 159, 145104 (2023)
https://doi.org/10.1063/5.0171700

The Journal of Chemical Physics ARTICLE pubs.aip.org/aip/jcp

Conditions for EPR detection of chirality-induced spin selectivity in spin-polarized radical pairs in isotropic solution

Cite as: J. Chem. Phys. 159, 145104 (2023); doi: 10.1063/5.0171700
Submitted: 10 August 2023 • Accepted: 19 September 2023 •
Published Online: 11 October 2023

Yi Ren and P. J. Hore[a)]

AFFILIATIONS

Department of Chemistry, University of Oxford, Oxford, United Kingdom

[a)]Author to whom correspondence should be addressed: peter.hore@chem.ox.ac.uk

ABSTRACT

Chiral molecules can act as spin filters, preferentially transmitting electrons with spins polarized along their direction of travel, an effect known as chirality-induced spin selectivity (CISS). In a typical experiment, injected electrons tunnel coherently through a layer of chiral material and emerge spin-polarized. It is also possible that spin polarization arises in radical pairs formed photochemically when electrons hop incoherently between donor and acceptor sites. Here we aim to identify the magnetic properties that would optimise the visibility of CISS polarization in time-resolved electron paramagnetic resonance (EPR) spectra of transient radical pairs without the need to orient or align their precursors. By simulating spectra of actual and model systems, we find that CISS contributions to the polarization should be most obvious when at least one of the radicals has small g-anisotropy and an inhomogeneous linewidth larger than the dipolar coupling of the two radicals. Under these conditions there is extensive cancellation of absorptive and emissive enhancements making the spectrum sensitive to small changes in the individual EPR line intensities. Although these cancellation effects are more pronounced at lower spectrometer frequencies, the spectral changes are easier to appreciate with the enhanced resolution afforded by high-frequency EPR. Consideration of published spectra of light-induced radical pairs in photosynthetic bacterial reaction centres reveals no significant CISS component in the polarization generated by the conventional spin-correlated radical pair mechanism.

I. INTRODUCTION

Spin-polarized radical pairs are formed in photochemical reactions when electrons hop incoherently between donor and acceptor molecules.[1–6] The origin of the spin polarization, which has been studied by a variety of electron paramagnetic resonance (EPR) techniques,[7–9] lies in the spin-conserving nature of electron transfer in molecules lacking the heavy atoms that would confer strong spin–orbit coupling. For example, charge separation from a photo-excited singlet-state donor to a closed-shell acceptor, or series of acceptors, forms radical pairs spin-selectively as electronic singlets. With spin energy-level populations far from thermal equilibrium, radical pairs show strong and distinctive EPR signatures from which information on the structure, kinetics, energetics and magnetic properties of the radicals can be extracted.[6]

Another potential source of spin polarization in photo-induced radical pairs is the phenomenon known as chirality-induced spin selectivity (CISS) in which chiral molecules act as spin filters, preferentially transmitting electrons with spins polarized along their direction of motion.[10–15] In a typical experiment, injected electrons tunnel coherently through a layer of chiral material and emerge spin-polarized. Although there are good reasons to think that CISS polarization should also arise in radical pairs formed by photo-induced electron hopping,[16–18] and that it should be detectable by EPR,[19–22] this has yet to be demonstrated unambiguously. Using a spintronic detection device, Carmeli *et al.* have reported spin-selective passage of electrons through a monolayer of oriented photosystem I reaction centres in what appears to be a CISS mechanism operating on the electron transfer pathway within the protein.[23] In a time-resolved EPR study, Privitera *et al.* observed spin polarization

generated by photo-induced charge transfer from a quantum dot to C_{60} via a helical oligopeptide bridge but were unable to prove unambiguously that it was a CISS effect.[21] On the theoretical side, several authors have discussed the conditions under which CISS polarization could be convincingly identified by EPR[16,19,20] and whether CISS could play a role in the proposed cryptochrome mechanism of avian magnetoreception.[19,24,25] Finally, Fay and Limmer have put forward a mechanism by which CISS polarization should arise in radical pairs formed by sequential electron transfers from an excited singlet-state donor to consecutive acceptors:[17]

$$D^{*}A_1A_2 \rightarrow D^{\bullet+}A_1^{\bullet-}A_2 \rightarrow D^{\bullet+}A_1A_2^{\bullet-}. \tag{1}$$

The authors predicted how the CISS polarization in $D^{\bullet+}A_1A_2^{\bullet-}$ depends on the initial spin state and exchange interaction in $D^{\bullet+}A_1^{\bullet-}A_2$, the rate constant for its conversion to $D^{\bullet+}A_1A_2^{\bullet-}$, and details of the electron transfer process and the spin–orbit coupling.[17] The aforementioned radical pairs, in photosystem I and the quantum dot-bridge-C_{60} molecule, are both formed via intermediate charge transfer states, as per Eq. (1).[21,23]

The nature of the CISS effect is that, other things being equal, the polarizations generated by electron transfer along antiparallel paths should be identical in magnitude and of opposite sign. It might be thought, therefore, that there would be no observable polarization for an isotropic ensemble in which antiparallel orientations of radical pairs are equally likely. This appears to be the case when the two unpaired electrons have exclusively isotropic spin-spin interactions: spherical averaging should cause any CISS contribution to the spin polarization to reduce to a uniform scaling of the amplitude of the whole spectrum making it difficult to assess the extent or even the existence of a CISS effect.[19] However, as argued by Chiesa *et al.*, this is not true of an EPR experiment on dipolar-coupled radical pairs.[20] CISS effects may then survive spherical averaging because EPR signals with equal and opposite polarizations do not necessarily appear at the same position in the spectrum so that cancellation is no longer complete.

In this report, we start from the premise that CISS polarization does indeed arise in radical pairs formed in photoinduced electron transfer reactions and aim to identify the magnetic properties that would optimise its visibility in time-resolved EPR spectra without the need to orient or align the reactants.

II. EPR SIMULATIONS

Continuous-wave, time-resolved EPR spectra were simulated using an approach[2,4,26,27] previously employed to interpret spectra of light-induced spin-correlated radical pairs (SCRPs) in photosynthetic reaction centre proteins[2,4,26,28–32] and in a variety of model compounds.[6,33–35] Briefly, the amplitudes of individual EPR transitions are calculated as the products of their polarizations and their transition probabilities; spin coherences are ignored by virtue of fast dephasing, interference effects, and experimental timing; hyperfine interactions are assumed to give rise to isotropic inhomogeneous line-broadening; spin-lattice relaxation is assumed to be too slow to affect the observed polarizations; and molecular motion is ignored.[2,4,26,27]

Simulations were based on the four-level system comprising the high-field spin states of the unpaired electrons in radicals labelled P and Q:

$$\begin{aligned} |1\rangle &= |\alpha_P\alpha_Q\rangle = |T_{+1}\rangle \\ |2\rangle &= \cos\psi|S\rangle + \sin\psi|T_0\rangle \\ |3\rangle &= -\sin\psi|S\rangle + \cos\psi|T_0\rangle \\ |4\rangle &= |\beta_P\beta_Q\rangle = |T_{-1}\rangle \end{aligned} \tag{2}$$

where $|S\rangle = \frac{1}{\sqrt{2}}|\alpha_P\beta_Q\rangle - \frac{1}{\sqrt{2}}|\beta_P\alpha_Q\rangle$ and $|T_0\rangle = \frac{1}{\sqrt{2}}|\alpha_P\beta_Q\rangle + \frac{1}{\sqrt{2}}|\beta_P\alpha_Q\rangle$, with α and β denoting the $m = +1/2$ and $m = -1/2$ electron spin states, respectively. The mixing angle ψ characterises the coupling of the two spins (of which more below). For each orientation of the radical pair, a stick spectrum was constructed by calculating the magnetic fields, B_{jk}, at which the four allowed EPR transitions ($|k\rangle \rightarrow |j\rangle$) occur and assigning them amplitudes, I_{jk}, equal to the appropriate population differences scaled by the corresponding transition probabilities:

$$I_{jk} = t_{jk}(p_k - p_j);\ jk \in \{12, 34, 13, 24\};\ \sum_{k=1}^{4} p_k = 1. \tag{3}$$

The four line positions, B_{jk}, are the solutions of:[4]

$$\begin{aligned} \omega &= \frac{1}{2}(g_P + g_Q)\mu_B B_{12}/\hbar - \sqrt{\left(J + \frac{1}{2}D_{zz}\right)^2 + \Delta_{12}^2} - (J - D_{zz}), \\ \omega &= \frac{1}{2}(g_P + g_Q)\mu_B B_{34}/\hbar - \sqrt{\left(J + \frac{1}{2}D_{zz}\right)^2 + \Delta_{34}^2} + (J - D_{zz}), \\ \omega &= \frac{1}{2}(g_P + g_Q)\mu_B B_{13}/\hbar + \sqrt{\left(J + \frac{1}{2}D_{zz}\right)^2 + \Delta_{13}^2} - (J - D_{zz}), \\ \omega &= \frac{1}{2}(g_P + g_Q)\mu_B B_{24}/\hbar + \sqrt{\left(J + \frac{1}{2}D_{zz}\right)^2 + \Delta_{24}^2} + (J - D_{zz}), \end{aligned} \tag{4}$$

and the transition probabilities, t_{jk}, are:[4]

$$t_{12} = t_{24} = \sin^2\psi;\ t_{13} = t_{34} = \cos^2\psi \tag{5}$$

with:

$$D_{zz} = D\left(\cos^2\xi - \frac{1}{3}\right) \tag{6}$$

$$\Delta_{jk} = \frac{1}{2}(g_P - g_Q)\mu_B B_{jk}/\hbar \tag{7}$$

$$g_K = \sqrt{\sum_{q\in\{x,y,z\}} (g_{Kq})^2 \cos^2\theta_{Kq}};\quad K \in \{P,Q\} \tag{8}$$

$$\psi = \frac{1}{2}\arctan\left(\frac{\frac{1}{2}(g_P - g_Q)\mu_B\overline{B}/\hbar}{J + 1/2D_{zz}}\right) \tag{9}$$

$$\overline{B} = \frac{1}{4}\sum_{jk} B_{jk}. \tag{10}$$

ω is the EPR spectrometer frequency; J and D are, respectively, the strengths of the exchange and dipolar interactions; ξ is the angle

between the magnetic field and the dipolar axis; g_{Kq} and θ_{Kq} are, respectively, the principal components of the g-tensors and the angles between the magnetic field vector and the principal axes of the g-tensors.

In the conventional SCRP model, for a radical pair formed in a singlet state, the fractional populations of the four spin states are independent of orientation:

$$p_1 = p_4 = 0;\ p_2 = \cos^2\psi;\ p_3 = \sin^2\psi \tag{11}$$

giving EPR intensities:[4]

$$I_{12} = I_{13} = -I_{24} = -I_{34} = \sin^2\psi\cos^2\psi \tag{12}$$

In this case, with no CISS polarization, each single-orientation stick spectrum comprises two antiphase doublets [Fig. 1(a)]. The phase of this multiplet polarization for a singlet-born pair (EA or AE, reading from low field to high, where E and A denote emission and absorption, respectively) is determined by the sign of $J - D_{zz}$.[4]

CISS polarization was incorporated phenomenologically[19] by writing the initial density operator of the radical pair, $|\Phi_\parallel\rangle\langle\Phi_\parallel|$, as a superposition of $|\mathrm{S}\rangle$ and $|\mathrm{T}_0\rangle$:

$$|\Phi_\parallel\rangle = \cos\left(\frac{\chi}{2}\right)|\mathrm{S}\rangle + \sin\left(\frac{\chi}{2}\right)|\mathrm{T}_0\rangle \tag{13}$$

where the $\parallel$ subscript indicates that the magnetic field is parallel to the CISS polarization axis. When $\chi = 0$, the radical pair is formed in a singlet state with pure SCRP polarization (no CISS). In the other extreme, of 100% CISS polarization, $\chi = \pm\pi/2$ and the initial state is either $|\alpha_P\beta_Q\rangle\langle\alpha_P\beta_Q|$ or $|\beta_P\alpha_Q\rangle\langle\beta_P\alpha_Q|$, depending on the sign of χ. In practice, the magnitude and sign of χ would be determined by a number of factors including spin–orbit coupling and the chiral properties of the medium through which the electron is transferred when the radical pair is formed.[16–18] For simplicity, the CISS polarization axis was assumed to be parallel to the dipolar axis (the vector connecting the centres of spin density of the two radicals). From Eq. (13), when the CISS axis is aligned with the magnetic field ($\xi = 0$), the initial polarization is given by the density operator:[19]

$$|\Phi_\parallel\rangle\langle\Phi_\parallel| = \frac{1}{4}\hat{E} - \hat{S}_{Pz}\hat{S}_{Qz} + \frac{1}{2}\left(\hat{S}_{Pz} - \hat{S}_{Qz}\right)\sin\chi \tag{14}$$

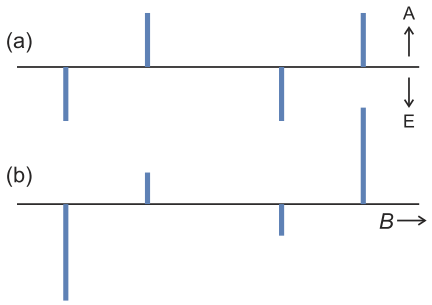

FIG. 1. Schematic spin-polarized EPR spectra of a pair of coupled electron spins with no hyperfine interactions. The horizontal axis is the magnetic field strength, B. (a) EA-EA polarization pattern expected for a radical pair formed in a pure singlet state with $J - D_{zz} > 0$. (b) A CISS contribution adds equal and opposite net polarizations for the two spins, here EE-AA, distorting the inversion symmetry of the antiphase doublets in (a).

where $\hat{E}$ is the identity operator, $\hat{S}_{Pz}$ and $\hat{S}_{Qz}$ are spin operators, and the third term is the CISS contribution.

In the general case ($\xi \neq 0$), the fractional populations of the four energy levels are (Appendix A):

$$\begin{aligned} p_1 = p_4 &= \frac{1}{2}\left[\sin\left(\frac{\chi}{2}\right)\sin(\xi)\right]^2, \\ p_2 &= \left[\sin\left(\frac{\chi}{2}\right)\sin(\psi)\cos(\xi) + \cos\left(\frac{\chi}{2}\right)\cos(\psi)\right]^2, \\ p_3 &= \left[\sin\left(\frac{\chi}{2}\right)\cos(\psi)\cos(\xi) - \cos\left(\frac{\chi}{2}\right)\sin(\psi)\right]^2. \end{aligned} \tag{15}$$

The resulting stick spectrum [Fig. 1(b)] is now composed of the multiplet (antiphase) SCRP polarization [Fig. 1(a)] superimposed on a net (in-phase) CISS polarization with equal and opposite amplitudes for the two spins. The phase of this polarization is determined by the sign of χ, i.e. whether the CISS effect favours population of $|\alpha_P\beta_Q\rangle$ or $|\beta_P\alpha_Q\rangle$.

Finally, the total stick spectrum of a randomly oriented ensemble of radical pairs was calculated by summing the individual stick spectra over an isotropic distribution of magnetic field directions, and modelling the unresolved hyperfine interactions by inhomogeneous line-broadening. The latter was implemented by convolving the total stick spectrum with the Gaussian function, $f(B) = \sqrt{2/(\pi\Delta B^2)}\exp\left[-2(B/\Delta B)^2\right]$, in which the linewidth, ΔB, is the separation of the points of inflection or, equivalently, twice the standard deviation of $f(B)$. For simplicity, the two radicals are assumed to have the same ΔB.

III. RESULTS

A. Dipolar-coupled radical pairs

Figure 2 shows the appearance of one of the EPR doublets of a prototype dipolar-coupled radical pair as a function of the magnetic field direction, ξ, for five values of χ. Here, the electrons were treated as weakly coupled (i.e. $\frac{1}{2}|g_P - g_Q|\mu_B\overline{B}/\hbar \gg |J + \frac{1}{2}D_{zz}|$), the g-tensor was isotropic, and there was no exchange interaction ($J = 0$). The χ-values were chosen to give evenly spaced values of $X = 1 - \cos\chi$ in the range $0 \leq X \leq 1$. We refer to X as the "CISS fraction" (see Appendix B for a justification of this choice). $X = 0$ denotes no CISS, and $X = 1$ corresponds to 100% CISS polarization.

The positions of the two lines are determined by the dipolar splitting via Eq. (6). As the CISS fraction is increased, the antiphase structure of the doublet becomes distorted such that the two components no longer have equal and opposite polarizations (cf. Fig. 1). When the field is aligned with the CISS/dipolar axis ($\xi = 0$ or $\xi = \pi$) and $X = 1$, one of the two components has zero intensity, consistent with the exclusive population of the $|\alpha_P\beta_Q\rangle$ or $|\beta_P\alpha_Q\rangle$ energy level.

When the spectra in Fig. 2 are averaged over ξ for an isotropic distribution of radical pairs, the result for $X = 0$ (i.e. no CISS) is the expected EAEA (antiphase Pake doublet) pattern, Fig. 3(a).[4] As the CISS contribution is increased, the central AE components weaken and eventually change sign to give an EEAA antiphase doublet when $X = 1$, Fig. 3(a). For comparison, Fig. 3(b) shows the corresponding spectra for a non-zero (isotropic) exchange interaction with no dipolar coupling. In this case, where the CISS polarization is the only

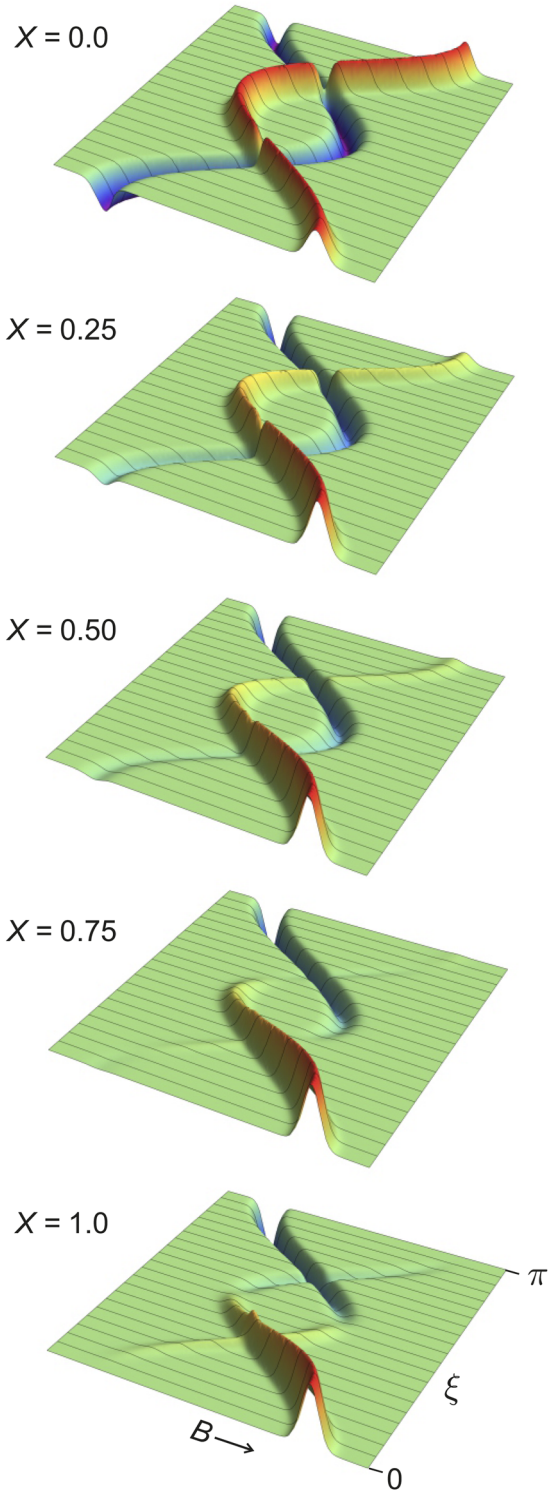

FIG. 2. Schematic spin-polarized EPR spectra of one of the doublets of a dipolar-coupled pair of electron spins. Spectra are shown as a function of orientation, $0 \le \xi \le \pi$, for CISS fractions, X, between 0 and 1, as indicated. $D < 0$ and $\Delta B = |D|/10$.

source of anisotropy, the EA doublet pattern is independent of X and the only change is a $(1 - 2X/3)$ scaling of the intensity of the whole spectrum.

The reason that the CISS polarization survives spherical averaging when $D \neq 0$ is that the positions of the lines in the spectrum, as well as the polarizations, depend on the direction of the magnetic field with respect to the radical pair (Fig. 2). Given the long-range nature of the dipolar interaction, it is unlikely in practice that any CISS contribution to the EPR spectrum would *completely* cancel for an isotropic collection of radical pairs.

As noted by Chiesa *et al.*,[20] the spectrum of an isotropic ensemble is insensitive to the sign of χ, i.e. enantiomers should have identical spectra. Fundamentally this stems from the property of the line intensities that $I_{jk}(\xi,\chi) = I_{jk}(\pi - \xi, -\chi)$ and because the line positions, B_{jk}, are unchanged by exact inversion of the magnetic field direction relative to the radical pair.

B. Radical pairs in bacterial photosynthetic reaction centres

For a real example, we turn to the radical pair formed by light-irradiation of deuterated, Zn-substituted reaction centre proteins of the photosynthetic bacterium *Rhodobacter sphaeroides* R-26, studied by Bittl, van der Est, Lubitz, Möbius, Prisner, Stehlik and colleagues in the 1990s.[28–30] Excitation of the primary electron donor, P_{865}, a bacteriochlorophyll dimer, induces an electron to hop via an intermediary acceptor to a ubiquinone-10 acceptor, Q_A, forming the radical pair $[P_{865}^{\bullet+}Q_A^{\bullet-}]$. Samples were extensively studied using time-resolved, field-swept EPR techniques at X-band (~9 GHz), K-band (~24 GHz) and W-band (~95 GHz) frequencies. Deuteration was used to reduce the inhomogeneous line-broadening arising from unresolved hyperfine interactions.

The majority of the parameters needed for analysis of the spin-polarized $[P_{865}^{\bullet+}Q_A^{\bullet-}]$ spectra had been determined independently from the crystal structure of the ground state protein and from high-field continuous-wave EPR.[28,30,36–38] Prisner *et al.*[30] obtained very satisfactory simulations using the SCRP simulation method described above, without considering CISS (which was only reported for the first time a few years later[39]). With the exception of the inhomogeneous line-width (different for protonated and deuterated samples), a single set of parameters accounted for all spectra at all three EPR frequencies giving considerable confidence that the SCRP model is more than adequate to account quantitatively for the polarization of $[P_{865}^{\bullet+}Q_A^{\bullet-}]$ in this protein complex.[30]

Figure 4(b) shows simulations of the X-band, K-band and W-band spectra of the deuterated radical pairs using the parameters of the original analysis[30] and the method outlined above.[2,4] The violet traces ($X = 0$) replicate the published simulations which in turn agree well with the reported experimental spectra (not shown).[30] As can be seen from the thermally polarized spectra of the two radicals in Fig. 4(a), $P_{865}^{\bullet+}$ and $Q_A^{\bullet-}$ contribute mainly to the high- and low-field regions, respectively, with a greater degree of overlap at the lower spectrometer frequencies.

The changes in the spectra as the CISS fraction is increased are visible in Fig. 4 at all three frequencies but are most pronounced at X-band, presumably because the lower spectral resolution leads to more severe cancellation of E and A contributions, and hence

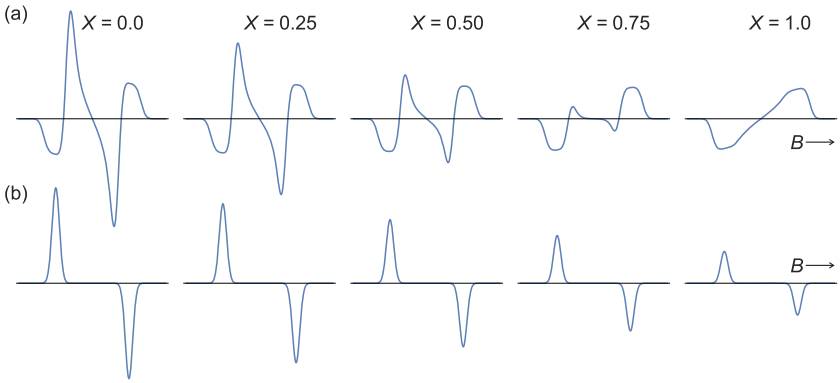

FIG. 3. (a) Isotropic averages of the spectra shown in Fig. 2 for CISS fractions, X, between 0 and 1, as indicated. $D = -1$ (arbitrary units) and $\Delta B = |D|/10$. (b) The same as (a) except that $D = 0$, $J = -0.5$ (same arbitrary units) and $\Delta B = |J|/5$.

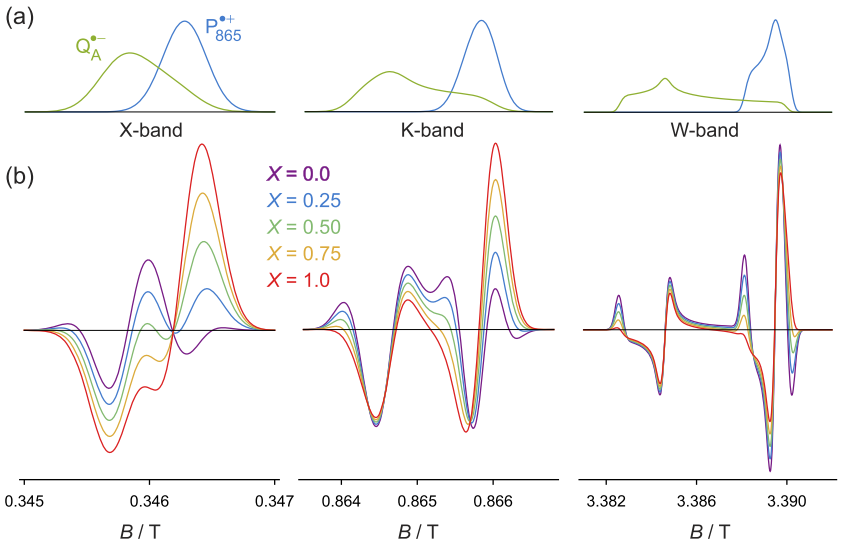

FIG. 4. Simulated EPR spectra of deuterated, Zn-substituted reaction centres of *Rhodobacter sphaeroides* R-26 at X-band (9.213 65 GHz), K-band (24.269 47 GHz) and W-band (95.0 GHz). (a) Spectra of the separate, thermally polarized $P_{865}^{\bullet+}$ and $Q_A^{\bullet-}$ radicals (high-temperature approximation). (b) Spin-polarized spectra for CISS fractions between 0 and 1, as indicated. Parameters: $g_{Px} = 2.0033$, $g_{Py} = 2.0025$, $g_{Pz} = 2.0021$, $g_{Qx} = 2.0066$, $g_{Qy} = 2.0054$, $g_{Qz} = 2.0022$, $J = 0$, $D = -0.124$ mT, $\Delta B = 0.315$ mT. The Euler angles defining the orientation of $\mathbf{g}_P$ relative to $\mathbf{g}_Q$ were $\alpha_P = 23.0°$, $\beta_P = 119.3°$, $\gamma_P = 18.3°$, and the polar angles that specify the dipolar axis relative to $\mathbf{g}_Q$ were $\theta_D = 71.6°$, $\phi_D = 68.5°$. The linewidth used here, ΔB, was the mean of those used in the original work ($\Delta B_P = 0.33$ mT, $\Delta B_Q = 0.30$ mT).[30]

greater sensitivity to small changes in the individual transition intensities. This is confirmed by Fig. 5 which shows the total spectrum of $[P_{865}^{\bullet+}Q_A^{\bullet-}]$ (black) as the sum of $I_{12} + I_{34}$ (red) and $I_{13} + I_{24}$ transitions (green). The former arises mostly from $P_{865}^{\bullet+}$, the latter mostly from $Q_A^{\bullet-}$. This assignment is only approximate because the spins are not strictly in the weak coupling limit ($\frac{1}{2}|g_P - g_Q|\mu_B\overline{B}/\hbar \gg |J + \frac{1}{2}D_{zz}|$). As an aside, we note that although the weak coupling approximation appears to work well in the absence of CISS, even at X-band, it does a poor job of reproducing the exact simulations when CISS polarization is included, especially at X-band. For this reason, the weak coupling approximation was not used for the simulations presented in Figs. 4–6.

As the CISS fraction was increased from 0 to 0.15, the $Q_A^{\bullet-}$ component in Fig. 5 hardly changed. Almost all of the dependence on X comes in the high-field region and stems from $P_{865}^{\bullet+}$ probably as a result of its smaller g-anisotropy and hence more extensive cancellation of E and A polarizations.

C. Model radical pairs

The conditions required for a small CISS polarization to make a large difference to the spectrum of a spin-correlated radical pair can be seen more clearly still from Fig. 6 which shows W-band simulations of a model dipolar-coupled radical pair in which one

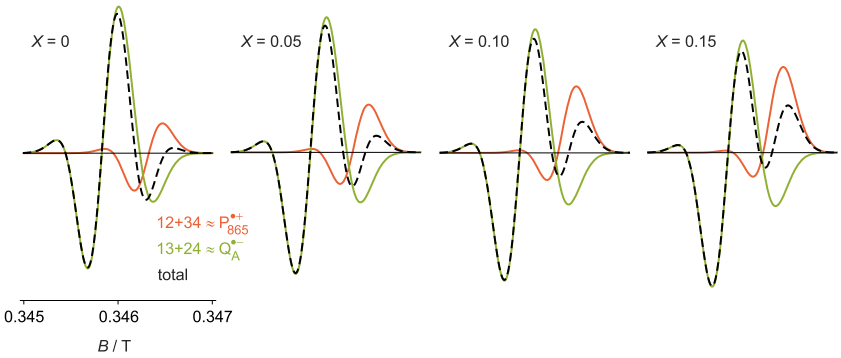

FIG. 5. Simulated spin-polarized EPR spectra of deuterated, Zn-substituted reaction centres of *Rhodobacter sphaeroides* R-26 at X-band (9.213 65 GHz) for CISS fractions between 0 and 0.15, as indicated. Red: sum of 12 and 34 transitions. Green: sum of 13 and 24 transitions. Black: sum of all four contributions. Same parameters as Fig. 4. All four plots have the same vertical scale.

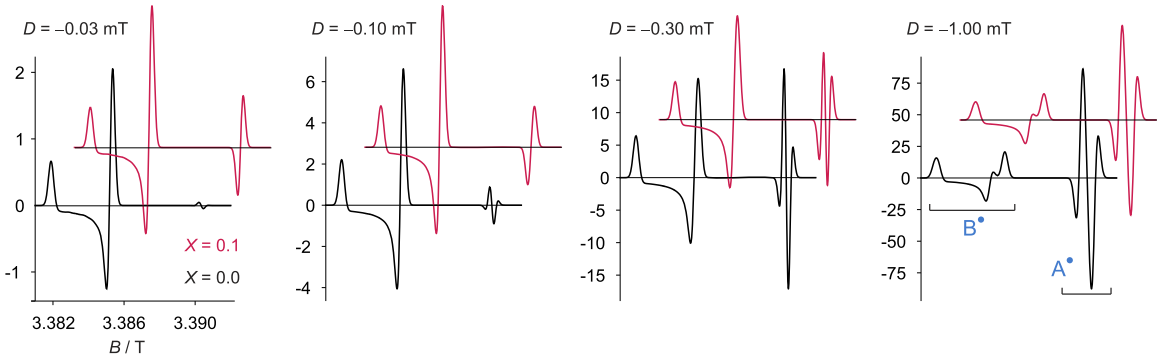

FIG. 6. Simulated spin-polarized EPR spectra of a model radical pair at W-band (95.0 GHz) for dipolar couplings between −0.03 and −1.00 mT, and CISS fractions of 0 (black) and 0.1 (red) as indicated. Parameters: $g_{Ax} = g_{Ay} = g_{Az} = 2.0020$, $g_{Bx} = 2.0070$, $g_{By} = g_{Bz} = 2.0050$, $J = 0$, $\Delta B = 0.3$ mT. $\alpha_A = \beta_A = \gamma_A = 0$, $\theta_D = 20°$, $\phi_D = 0$. The dipolar couplings correspond to radical-radical separations of 4.5, 3.0, 2.1 and 1.4 nm. The $X = 0.1$ spectra have been offset for clarity.

radical ($A^\bullet$) has an isotropic g-tensor and the other ($B^\bullet$) an axial g-tensor. Calculated spectra are shown for four values of the dipolar coupling, with $X = 0.0$ and $X = 0.1$. The spectral features at 3.3819 and 3.3853 T come from $B^\bullet$ and those at 3.3903 T from $A^\bullet$. As D is increased, both the intensity and the resolution of the $X = 0.0$ spectra increase as a result of the reduced overlap and consequent cancellation of E and A polarizations.

The spectrum of $A^\bullet$ is much more sensitive to a 10% CISS fraction than that of $B^\bullet$. In particular, when D is smaller than the linewidth (0.3 mT), one sees dramatic changes in the amplitude and shape of the $A^\bullet$ spectrum: a small CISS contribution changes its EAEA pattern to EA (most easily seen for $D = -0.10$ mT). This occurs because an increase in X weakens the inner (AE) peaks of the EAEA pattern and strengthens the outer (EA) peaks such that, when broadened, the inner peaks tend to cancel, allowing the outer peaks to dominate. The form of the $A^\bullet$ spectrum ceases to be so sensitive to D as soon as dipolar splitting is well resolved ($|D| \geq 0.3$ mT). By contrast, the shapes of the $B^\bullet$ spectra, which are much broader because of the g-anisotropy, are essentially the same for $X = 0$ and $X = 0.1$.

IV. DISCUSSION

The aim of the simulations presented above was to identify the magnetic properties that would maximize the visibility of CISS polarization in the EPR spectrum of randomly oriented spin-correlated radical pairs. To do this we have used a well-established spectral simulation procedure,[4] with CISS polarization incorporated phenomenologically.[19] Experimental conditions were considered in which zero-quantum coherence is not detected, such that the EPR spectrum reflects the initial polarizations of the coupled radicals. As a consequence of this approximation, the validity of the simulations presented here is not restricted to our choice of initial state.[19] Völker *et al.*[22] have suggested a more general form of Eq. (13), which allows for all possible superpositions of $|S\rangle$ and $|T_0\rangle$:

$$|\Phi_\parallel\rangle = \cos\alpha\,|S\rangle + e^{i\beta}\sin\alpha\,|T_0\rangle \tag{16}$$

and corresponds to the density operator

$$|\Phi_{\parallel}\rangle\langle\Phi_{\parallel}| = \frac{1}{4}\hat{E} - \hat{S}_{Pz}\hat{S}_{Qz} + \frac{1}{2}\left(\hat{S}_{Pz} - \hat{S}_{Qz}\right)\sin 2\alpha\,\cos\beta - ZQ_x\,\cos 2\alpha + ZQ_y\,\sin 2\alpha\,\sin\beta \quad (17)$$

where the zero-quantum operators are:[40]

$$ZQ_x = \hat{S}_{Px}\hat{S}_{Qx} + \hat{S}_{Py}\hat{S}_{Qy}; \quad ZQ_y = \hat{S}_{Py}\hat{S}_{Qx} - \hat{S}_{Px}\hat{S}_{Qy}. \quad (18)$$

Discarding the coherent terms, Eq. (17) is identical to the form we have used, Eq. (14), if $\sin 2\alpha\cos\beta$ is identified with $\sin\chi$. Equation (14) is also consistent with the non-coherent, phenomenological density operator used by Chiesa *et al.*:[20]

$$\left(\frac{1+p}{2}\right)|\alpha_P\beta_Q\rangle\langle\alpha_P\beta_Q| + \left(\frac{1-p}{2}\right)|\beta_P\alpha_Q\rangle\langle\beta_P\alpha_Q| \quad (19)$$

with the replacement, $p = \sin\chi$. Furthermore, Eq. (17) has the same form as the density operator derived by Fay and Limmer[17] by considering consecutive charge transfer states, except that in their treatment, the amplitudes of the CISS polarization and the zero-quantum terms can be calculated from the properties of the radicals, the spin–orbit coupling, and the details of the electron transfer steps.

Prior to the first report of CISS, it was demonstrated that multifrequency EPR spectra of $[P^{\bullet+}_{865}Q^{\bullet-}_{A}]$ in bacterial reaction centres could be very satisfactorily simulated using the conventional SCRP model as the source of polarization.[30] This analysis was particularly convincing because so many of the required parameters were reliably known from independent measurements. Had there been a significant CISS polarization under the conditions of those experiments, it is unlikely (in our view) that such good agreement with experiment would have been obtained using a model that did not (and could not at that time) account for CISS. Although qualitatively, $[P^{\bullet+}_{865}Q^{\bullet-}_{A}]$ satisfies one of the conditions for non-zero CISS polarization (formation by sequential electron hopping[17]), its immediate precursor, $[P^{\bullet+}_{865}\Phi^{\bullet-}_{A}]$ (Φ_A is a bacteriopheophytin), may not have the properties required for a measurable CISS polarization in $[P^{\bullet+}_{865}Q^{\bullet-}_{A}]$ (Appendix C). The corresponding spin-correlated radical pair in plant photosystem I ($[P^{\bullet+}_{700}A^{\bullet-}_{1}]$) has also been extensively studied by EPR, again with no suggestion of a component in the polarization that could not be accounted for within the SCRP model.[41–45] However, these measurements are not directly comparable to the study of CISS in photosystem I by Carmeli *et al.*[23] and one can imagine several reasons for the discrepancy. First, the electron transfer pathway in photosystem I extends beyond the phylloquinone acceptor A_1 to the [4Fe 4S] iron-sulphur clusters F_X, F_A and F_B which might have contributed to the polarization. Second, the two experiments were done at different temperatures: Carmeli *et al.* report a maximum in the polarization at 300 K and a drop-off at lower temperatures, reaching zero by 150 K; the EPR measurements were done at 50–77 K.[42] Third, as Carmeli *et al.* acknowledge,[23] it is possible that polarization arises from the passage of electrons from the Fe–S clusters through the chiral protein. Fourth, the alignment of the proteins in Carmeli's study should enhance the effect by reducing the cancellation of absorptive and emissive contributions.

Many published studies of spin-polarized EPR spectra have focussed on radical pairs about which far less is known in advance than for $[P^{\bullet+}_{865}Q^{\bullet-}_{A}]$. If several of the simulation parameters can only be estimated by spectral fitting, there is a possibility that CISS polarization might have been mistaken for SCRP polarization, with the difference between the two obscured by the values of the parameters obtained by fitting. It seems clear that there is a better chance of identifying a (possibly small) CISS component if more parameters (*g*-tensors, dipolar and exchange interactions, relative orientations of radicals, etc.) are known in advance and fewer have to be determined by spectral analysis.

V. CONCLUSIONS

Consideration of the reported spectra of light-induced radical pairs in photosynthetic bacterial reaction centres[30] reveals no significant CISS component in the polarization generated by the conventional spin-correlated radical pair mechanism.

The main conclusion to be drawn from our simulations of randomly oriented, dipolar-coupled radical pairs is that if CISS does contribute to the polarization then it should be most obvious when at least one of the radicals has a small *g*-anisotropy and an inhomogeneous linewidth larger than the dipolar interaction. Under these conditions there is extensive cancellation of absorptive and emissive polarizations which makes the spectrum sensitive to small deviations in the individual EPR line intensities from those expected for pure SCRP polarization. Although these cancellation effects are more pronounced at lower spectrometer frequencies, the spectral changes are easier to appreciate with the enhanced resolution afforded by high-frequency EPR.

Undoubtedly, CISS polarization will be easier to detect in the EPR spectra of aligned samples than for isotropic solutions. Nevertheless, measurements on randomly aligned molecules have the merit of experimental simplicity and avoid the complication in spectral analysis that the degree and nature of the molecular alignment may not be well defined.

ACKNOWLEDGMENTS

P.J.H. is grateful to the European Research Council under the European Union's Horizon 2020 research and innovation programme, Grant Agreement No. 810002, Synergy Grant: *QuantumBirds*.

AUTHOR DECLARATIONS

Conflict of Interest

The authors have no conflicts to disclose.

Author Contributions

Yi Ren: Investigation (lead); Writing – review & editing (supporting). **P. J. Hore**: Conceptualization (lead); Writing – original draft (lead).

DATA AVAILABILITY

The data that support the findings of this study are available within the article.

APPENDIX A: ENERGY-LEVEL POPULATIONS

An outline derivation of the energy-level populations in Eq. (15) follows. The high-field spin Hamiltonian of the two coupled electrons, P and Q, is:

$$\hat{H} = \omega_P \hat{S}_{Pz} + \omega_Q \hat{S}_{Qz} - (J - D_{zz})\left(\frac{1}{2}\hat{E} + 2\sum_{k=x,y,z} \hat{S}_{Pk}\hat{S}_{Qk}\right) \quad \text{(A1)}$$

where all the symbols have been defined in the main text. From Eq. (13), the initial state of the spin system when the magnetic field is parallel to the CISS axis can be written as the vector:[19]

$$\mathbf{\Phi}_{\parallel} = \frac{1}{\sqrt{2}}\left(0, \cos\left(\frac{\chi}{2}\right), \sin\left(\frac{\chi}{2}\right), 0\right)^{\mathrm{T}} \quad \text{(A2)}$$

in the $\{T_{+1},\ S,\ T_0,\ T_{-1}\}$ basis from which:

$$\mathbf{\Phi}_{\parallel} = \frac{1}{\sqrt{2}}\left(0, \cos\left(\frac{\chi}{2}\right) + \sin\left(\frac{\chi}{2}\right), \sin\left(\frac{\chi}{2}\right) - \cos\left(\frac{\chi}{2}\right), 0\right)^{\mathrm{T}} \quad \text{(A3)}$$

in the $\{\alpha_P\alpha_Q,\ \alpha_P\beta_Q,\ \beta_P\alpha_Q,\ \beta_P\beta_Q\}$ basis. When the magnetic field makes an angle ξ with the CISS axis, the initial spin state becomes:[19]

$$\mathbf{\Phi} = \exp\left[-i\xi\left(\hat{S}_{Py} + \hat{S}_{Qy}\right)\right]\mathbf{\Phi}_{\parallel}. \quad \text{(A4)}$$

Transforming to the eigenbasis of $\hat{H}$, we have:

$$\mathbf{\Phi}_e = \frac{1}{\sqrt{2}}\begin{pmatrix} \sqrt{2} & 0 & 0 & 0 \\ 0 & \cos\psi + \sin\psi & \sin\psi - \cos\psi & 0 \\ 0 & \cos\psi - \sin\psi & \cos\psi + \sin\psi & 0 \\ 0 & 0 & 0 & \sqrt{2} \end{pmatrix}\mathbf{\Phi} \quad \text{(A5)}$$

from which the energy-level populations, p_k, may be obtained as:

$$p_k = \left|(\mathbf{\Phi}_e)_k\right|^2,\ k \in \{1,2,3,4\}. \quad \text{(A6)}$$

APPENDIX B: CISS FRACTION

In the main text, we have used $X = 1 - \cos\chi$ to denote the "CISS fraction," i.e. the degree to which CISS contributes to the spin polarization of the radical pair. The justification for this choice follows.

When there is no CISS, $\chi = 0$ and the initial state is $|\Phi_{SCRP}\rangle = |S\rangle$. When there is 100% CISS and $\chi = \pi/2$, the initial state is $|\Phi_{CISS}\rangle = [|S\rangle + |T_0\rangle]/\sqrt{2} = |\alpha\beta\rangle$ (omitting the P and Q labels). For intermediate situations, we can write the initial spin state as a superposition of $|\Phi_{SCRP}\rangle$ and $|\Phi_{CISS}\rangle$ with real-valued coefficients, a and b:

$$|\Phi\rangle = a|\Phi_{SCRP}\rangle + b|\Phi_{CISS}\rangle = \left(a + \frac{b}{\sqrt{2}}\right)|S\rangle + \frac{b}{\sqrt{2}}|T_0\rangle \quad \text{(B1)}$$

where $b^2\ (= 1 - a^2)$ is interpreted as the CISS fraction, X. Comparing Eq. (B1) with Eq. (13) gives:

$$X = b^2 = 2\sin^2\left(\frac{\chi}{2}\right) = 1 - \cos\chi. \quad \text{(B2)}$$

APPENDIX C: ESTIMATE OF CISS POLARIZATION IN BACTERIAL REACTION CENTRES

Fay and Limmer[17] give the following expression for the CISS polarization of a radical pair formed by two sequential electron transfers (corresponding to $P^*_{865} \rightarrow [P^{\bullet+}_{865}\Phi^{\bullet-}_A] \rightarrow [P^{\bullet+}_{865}Q^{\bullet-}_A]$ in bacterial reaction centres, where P^*_{865} is the photo-excited singlet state of P_{865}):

$$P = -\frac{2J_{P\Phi}k_{PQ}\ \sin 2\theta}{k_{PQ}^2 + 4J_{P\Phi}^2 + \delta\varepsilon^2 + 4J_{P\Phi}\delta\varepsilon\ \cos 2\theta}. \quad \text{(C1)}$$

$J_{P\Phi}$ is the exchange interaction in $[P^{\bullet+}_{865}\Phi^{\bullet-}_A]$, k_{PQ} is the rate constant for the second electron transfer, $[P^{\bullet+}_{865}\Phi^{\bullet-}_A] \rightarrow [P^{\bullet+}_{865}Q^{\bullet-}_A]$, and the mixing angle θ depends on the relative sizes of the diabatic coupling ($V_{P\Phi}$) for the first electron transfer and the spin–orbit coupling ($\Lambda_{P\Phi}$). The "shift term" $\delta\varepsilon$ is a function of $V_{P\Phi}$, $\Lambda_{P\Phi}$, the reorganization energy and the thermodynamic driving force for $P^*_{865}\Phi_A \rightarrow [P^{\bullet+}_{865}\Phi^{\bullet-}_A]$.

The lifetime of $[P^{\bullet+}_{865}\Phi^{\bullet-}_A]$ in Zn-substituted reaction centres of *Rhodobacter sphaeroides* is 255 ps,[46] giving $k_{PQ} = 3.9 \times 10^9\ s^{-1}$ and the exchange interaction is −0.9 mT,[47] so that $J_{P\Phi} = -1.6 \times 10^8\ s^{-1}$. With these values, the maximum polarization, $P \approx 0.08$, occurs when $\theta = \pi/4$ and $\delta\varepsilon = 0$. This value corresponds to $\chi \approx 5°$ and $X \approx 0.003$. The polarization is small because, with $|k_{PQ}/J_{P\Phi}| \approx 24$, there is little time for the exchange interaction to change the phase of the singlet-triplet coherence in $[P^{\bullet+}_{865}\Phi^{\bullet-}_A]$ before it reacts to form $[P^{\bullet+}_{865}Q^{\bullet-}_A]$.[17] P would be more than an order of magnitude smaller for $\theta = \pi/4$ and $|\delta\varepsilon| = 10$ μeV.

REFERENCES

[1] M. C. Thurnauer and J. R. Norris, "An electron-spin echo phase-shift observed in photosynthetic algae: Possible evidence for dynamic radical pair interactions," Chem. Phys. Lett. **76**, 557 (1980).
[2] P. J. Hore, D. A. Hunter, C. D. McKie, and A. J. Hoff, "Electron paramagnetic resonance of spin-correlated radical pairs in photosynthetic reactions," Chem. Phys. Lett. **137**, 495 (1987).
[3] G. L. Closs, M. D. E. Forbes, and J. R. Norris, "Spin-polarized electron paramagnetic resonance spectra of radical pairs in micelles: Observation of electron spin-spin interactions," J. Phys. Chem. **91**, 3592 (1987).
[4] P. J. Hore, *Advanced EPR. Applications in Biology and Biochemistry*, edited by A. J. Hoff (Elsevier, Amsterdam, 1989), p. 405.
[5] K. L. Ivanov, A. Wagenpfahl, C. Deibel, and J. Matysik, "Spin-chemistry concepts for spintronics scientists," Beilstein J. Nanotechnol. **8**, 1427 (2017).
[6] S. M. Harvey and M. R. Wasielewski, "Photogenerated spin-correlated radical pairs: From photosynthetic energy transduction to quantum information science," J. Am. Chem. Soc. **143**, 15508 (2021).
[7] A. J. Hoff, *Advanced EPR. Applications in Biology and Biochemistry* (Elsevier, Amsterdam, 1989).
[8] K. Möbius and A. Savitsky, *High-field EPR Spectroscopy on Proteins and Their Model Systems* (Royal Society of Chemistry, Cambridge, UK, 2009).
[9] M. D. E. Forbes, L. E. Jarocha, S. Sim, and V. F. Tarasov, "Time-resolved electron paramagnetic resonance spectroscopy: History, technique, and application to supramolecular and macromolecular chemistry," Adv. Phys. Org. Chem. **47**, 1 (2013).
[10] R. Naaman, Y. Paltiel, and D. H. Waldeck, "Chiral induced spin selectivity gives a new twist on spin-control in chemistry," Acc. Chem. Res. **53**, 2659–2667 (2020).
[11] R. Naaman, Y. Paltiel, and D. H. Waldeck, "Chiral induced spin selectivity and its implications for biological functions," Annu. Rev. Biophys. **51**, 99 (2022).
[12] H. P. Lu, Z. V. Vardeny, and M. C. Beard, "Control of light, spin and charge with chiral metal halide semiconductors," Nat. Rev. Chem **6**, 470 (2022).

[13]C. D. Aiello, J. M. Abendroth, M. Abbas, A. Afanasev, S. Agarwal, A. S. Banerjee, D. N. Beratan, J. N. Belling, B. Berche, A. Botana, J. R. Caram, G. L. Celardo, G. Cuniberti, A. Garcia-Etxarri, A. Dianat, I. Diez-Perez, Y. Q. Guo, R. Gutierrez, C. Herrmann, J. Hihath, S. Kale, P. Kurian, Y. C. Lai, T. H. Liu, A. Lopez, E. Medina, V. Mujica, R. Naaman, M. Noormandipour, J. L. Palma, Y. Paltiel, W. Petuskey, J. C. Ribeiro-Silva, J. J. Saenz, E. J. G. Santos, M. Solyanik-Gorgone, V. J. Sorger, D. M. Stemer, J. M. Ugalde, A. Valdes-Curiel, S. Varela, D. H. Waldeck, M. R. Wasielewski, P. S. Weiss, H. Zacharias, and Q. H. Wang, "A chirality-based quantum leap," ACS Nano **16**, 4989 (2022).
[14]F. Evers, A. Aharony, N. Bar-Gill, O. Entin-Wohlman, P. Hedegård, O. Hod, P. Jelinek, G. Kamieniarz, M. Lemeshko, K. Michaeli, V. Mujica, R. Naaman, Y. Paltiel, S. Refaely-Abramson, O. Tal, J. Thijssen, M. Thoss, J. M. van Ruitenbeek, L. Venkataraman, D. H. Waldeck, B. Yan, and L. Kronik, "Theory of chirality induced spin selectivity: Progress and challenges," Adv. Mater. **34**, 2106629 (2022).
[15]A. Chiesa, A. Privitera, E. Macaluso, M. Mannini, R. Bittl, R. Naaman, M. R. Wasielewski, R. Sessoli, and S. Carretta, "Chirality-induced spin selectivity: An enabling technology for quantum applications," Adv. Mater. **35**, 2300472 (2023).
[16]T. P. Fay, "Chirality-induced spin coherence in electron transfer reactions," J. Phys. Chem. Lett. **12**, 1407 (2021).
[17]T. P. Fay and D. T. Limmer, "Origin of chirality induced spin selectivity in photoinduced electron transfer," Nano Lett. **21**, 6696 (2021).
[18]T. P. Fay and D. T. Limmer, "Spin selective charge recombination in chiral donor-bridge-acceptor triads," J. Chem. Phys. **158**, 194101 (2023).
[19]J. Luo and P. J. Hore, "Chiral-induced spin selectivity in the formation and recombination of radical pairs: Cryptochrome magnetoreception and EPR detection," New J. Phys. **23**, 043032 (2021).
[20]A. Chiesa, M. Chizzini, E. Garlatti, E. Salvadori, F. Tacchino, P. Santini, I. Tavernelli, R. Bittl, M. Chiesa, R. Sessoli, and S. Carretta, "Assessing the nature of chiral-induced spin selectivity by magnetic resonance," J. Phys. Chem. Lett. **12**, 6341 (2021).
[21]A. Privitera, E. Macaluso, A. Chiesa, A. Gabbani, D. Faccio, D. Giuri, M. Briganti, N. Giaconi, F. Santanni, N. Jarmouni, L. Poggini, M. Mannini, M. Chiesa, C. Tomasini, F. Pineider, E. Salvadori, S. Carretta, and R. Sessoli, "Direct detection of spin polarization in photoinduced charge transfer through a chiral bridge," Chem. Sci. **13**, 12208 (2022).
[22]L. A. Völker, K. Herb, E. Janitz, C. L. Degen, and J. M. Abendroth, "Toward quantum sensing of chiral induced spin selectivity: Probing donor-bridge-acceptor molecules with NV centers in diamond," J. Chem. Phys. **158**, 161103 (2023).
[23]I. Carmeli, K. S. Kumar, O. Heifler, C. Carmeli, and R. Naaman, "Spin selectivity in electron transfer in photosystem I," Angew. Chem., Int. Ed. **53**, 8953 (2014).
[24]Y. Tiwari and V. S. Poonia, "Role of chiral-induced spin selectivity in the radical pair mechanism of avian magnetoreception," Phys. Rev. E **106**, 064409 (2022).
[25]Y. Tiwari and V. S. Poonia, "Quantum coherence enhancement by the chirality-induced spin selectivity effect in the radical-pair mechanism," Phys. Rev. A **107**, 052406 (2023).
[26]D. Stehlik, C. H. Bock, and J. Petersen, "Anisotropic electron spin polarization of correlated spin pairs in photosynthetic reaction centers," J. Phys. Chem. **93**, 1612 (1989).
[27]C. E. Tait, M. D. Krzyaniak, and S. Stoll, "Computational tools for the simulation and analysis of spin-polarized EPR spectra," J. Magn. Reson. **349**, 107410 (2023).
[28]A. van der Est, R. Bittl, E. C. Abresch, W. Lubitz, and D. Stehlik, "Transient EPR spectroscopy of perdeuterated Zn-substituted reaction centers of *Rhodobacter sphaeroides* R-26," Chem. Phys. Lett. **212**, 561 (1993).
[29]G. Füchsle, R. Bittl, A. van der Est, W. Lubitz, and D. Stehlik, "Transient EPR spectroscopy of the charge separated state P^+Q^- in photosynthetic reaction centers. Comparison of Zn-substituted *Rhodobacter sphaeroides* R-26 and Photosystem-I," Biochim. Biophys. Acta, Bioenerg. **1142**, 23 (1993).
[30]T. F. Prisner, A. van der Est, R. Bittl, W. Lubitz, D. Stehlik, and K. Möbius, "Time-resolved W-band (95 GHz) EPR spectroscopy of Zn-substituted reaction centers of *Rhodobacter sphaeroides* R-26," Chem. Phys. **194**, 361 (1995).
[31]T. Berthold, E. Donner von Gromoff, S. Santabarbara, P. Stehle, G. Link, O. G. Poluektov, P. Heathcote, C. F. Beck, M. C. Thurnauer, and G. Kothe, "Exploring the electron transfer pathways in Photosystem I by high-time-resolution electron paramagnetic resonance: Observation of the B-Side radical pair $P_{700}{}^+A_{1B}{}^-$ in whole cells of the deuterated green alga *Chlamydomonas reinhardtii* at cryogenic temperatures," J. Am. Chem. Soc. **134**, 5563 (2012).
[32]K. Mobius and A. Savitsky, "High-field/high-frequency EPR spectroscopy in protein research: Principles and examples," Appl. Magn. Reson. **54**, 207 (2023).
[33]Z. B. Yu, A. A. Sukhanov, X. Xiao, A. Iagatti, S. Doria, V. Butera, J. Z. Zhao, V. K. Voronkova, M. Di Donato, and G. Mazzone, "Observation of long-lived charge-separated states in anthraquinone-phenothiazine electron donor-acceptor dyads: Transient optical and electron paramagnetic resonance spectroscopic studies," J. Phys. Chem. B **127**, 5905 (2023).
[34]A. Y. Lee, T. A. Colleran, A. Jain, J. Niklas, B. K. Rugg, T. Mani, O. G. Poluektov, and J. H. Olshansky, "Quantum dot-organic molecule conjugates as hosts for photogenerated spin qubit pairs," J. Am. Chem. Soc. **145**, 4372 (2023).
[35]F. B. Xie, H. C. Mao, C. J. Lin, Y. N. Feng, J. F. Stoddart, R. M. Young, and M. R. Wasielewski, "Quantum sensing of electric fields using spin-correlated radical ion pairs," J. Am. Chem. Soc. **145**, 14922 (2023).
[36]U. Ermler, G. Fritzsch, S. Buchanan, and H. Michel, *Research in Photosynthesis*, edited by N. Murata (Kluwer, Dordrecht, 1992).
[37]O. Burghaus, M. Plato, M. Rohrer, K. Moebius, F. Macmillan, and W. Lubitz, "3-mm high-field EPR on semiquinone radical-anions Q^- related to photosynthesis and on the primary donor P^+ and acceptor $Q_A{}^-$ in reaction centers of *Rhodobacter sphaeroides* R-26," J. Phys. Chem. **97**, 7639 (1993).
[38]R. Klette, J. T. Toerring, M. Plato, K. Moebius, B. Boenigk, and W. Lubitz, "Determination of the g tensor of the primary donor cation radical in single-crystals of *Rhodobacter sphaeroides* R-26 reaction centers by 3-mm high-field EPR," J. Phys. Chem. **97**, 2015 (1993).
[39]K. Ray, S. P. Ananthavel, D. H. Waldeck, and R. Naaman, "Asymmetric scattering of polarized electrons by organized organic films of chiral molecules," Science **283**, 814 (1999).
[40]O. W. Sorensen, G. W. Eich, M. H. Levitt, G. Bodenhausen, and R. R. Ernst, "Product operator formalism for the description of NMR pulse experiments," Prog. Nucl. Magn. Reson. Spectrosc. **16**, 163 (1984).
[41]S. G. Zech, W. Hofbauer, A. Kamlowski, P. Fromme, D. Stehlik, W. Lubitz, and R. Bittl, "A structural model for the charge separated state $P_{700}{}^+A_1{}^-$ in photosystem I from the orientation of the magnetic interaction tensors," J. Phys. Chem. B **104**, 9728 (2000).
[42]A. van der Est, T. Prisner, R. Bittl, P. Fromme, W. Lubitz, K. Mobius, and D. Stehlik, "Time-resolved X-K-and W-band EPR of the radical pair state $P_{700}{}^+A_1{}^-$ of photosystem I in comparison with $P_{865}{}^+Q_A{}^-$ in bacterial reaction centers," J. Phys. Chem. B **101**, 1437 (1997).
[43]A. Savitsky, J. Niklas, J. H. Golbeck, K. Mobius, and W. Lubitz, "Orientation resolving dipolar high-field EPR spectroscopy on disordered solids: II. Structure of spin-correlated radical pairs in photosystem I," J. Phys. Chem. B **117**, 11184 (2013).
[44]S. Santabarbara, I. Kuprov, W. V. Fairclough, S. Purton, P. J. Hore, P. Heathcote, and M. C. W. Evans, "Bidirectional electron transfer in photosystem I: Determination of two distances between $P_{700}{}^+$ and $A_1{}^-$ in spin-correlated radical pairs," Biochemistry **44**, 2119 (2005).
[45]S. Santabarbara, I. Kuprov, P. J. Hore, A. Casal, P. Heathcote, and M. C. W. Evans, "Analysis of the spin-polarized electron spin echo of the [$P700^+$ $A_1{}^-$] radical pair of photosystem I indicates that both reaction center subunits are competent in electron transfer in cyanobacteria, green algae, and higher plants," Biochemistry **45**, 7389 (2006).
[46]C. Kirmaier, D. Holten, R. J. Debus, G. Feher, and M. Y. Okamura, "Primary photochemistry of iron-depleted and zinc-reconstituted reaction centers from *Rhodopseudomonas sphaeroides*," Proc. Natl. Acad. Sci. U. S. A. **83**, 6407 (1986).
[47]I. I. Proskuryakov, I. B. Klenina, P. J. Hore, M. K. Bosch, P. Gast, and A. J. Hoff, "Electron paramagnetic resonance of the primary radical pair [$d^{\bullet+}$ $\varphi_a{}^{\bullet-}$] in reaction centers of photosynthetic bacteria," Chem. Phys. Lett. **257**, 333 (1996).